Letter to the Editor

Homing frequency of human T cells inferred from peripheral blood depletion kinetics after sphingosine-1-phosphate receptor blockade

To the Editor:

Naive and central memory (CM) T cells home through lymph nodes (LNs), whereas T cells with an effector memory (EM) phenotype preferentially screen peripheral tissues in search of cognate antigen.[1] LN entry and egress are distinct and highly regulated processes mediated by an orchestrated interplay of chemokines/chemokine receptors and adhesion molecules.[2] Interaction of peripheral node addressins with L-selectin on T cells allows tethering/rolling along high endothelial venules (HEVs).[2] Interaction of the chemokine receptor CCR7 with its ligands CCL19/CCL21 and CXCR4 with CXCL12 then mediates firm adhesion to HEVs through high-affinity interactions of lymphocyte function–associated antigen 1 and intercellular adhesion molecule 1, permitting transmigration of T cells across the HEV cell layer.[2] Within the LNs, T-cell migration is directed through T-cell zones toward the cortical sinuses.[3] A sphingosine-1-phosphate (S1P) gradient established across the endothelial cells of the cortical sinuses is directing LN egress of T cells through efferent lymph back to the peripheral blood circulation.[4] Acting as a functional antagonist on the S1P receptor, the pharmacologic compound fingolimod, which has shown efficacy in the treatment of multiple sclerosis (MS), blocks this egress.[4,5] As a consequence, in fingolimod-treated subjects naive and CM T cells are trapped in LNs and reduced in the blood circulation.[6]

Here, by studying depletion kinetics of T cells in the blood of *de novo* fingolimod-exposed subjects in combination with *in vitro* migration experiments, homing frequencies and LN access hierarchy between T-cell subsets were derived indirectly. First, we defined the effect of *de novo* fingolimod exposure on the number of circulating $CD4^+$ and $CD8^+$ phenotypic T-cell subsets in patients with MS during a 6-hour observation period (hourly measurements, 1 time before and 6 times after drug exposure) by using flow cytometry (detailed information on patients and methods is provided in the Methods section and Table E1 in this article's Online Repository at www.jacionline.org). In fingolimod-treated subjects, 6 hours after the first drug dose, numbers of $CD4^+$ T-cell subsets with an LN homing phenotype (ie, naive and CM T cells) were significantly reduced (Fig 1, *A* [representative example; absolute cell counts], and Fig 1, *B* [pooled data; proportional change]). Intriguingly, the kinetics of reduction differed between phenotypic naive (CD62 ligand [CD62L]–positive $CD45RA^+$) and CM ($CD62L^+CD45RA^-$) $CD4^+$ T cells. Specifically, compared with baseline measurements, naive $CD4^+$ T-cell counts started to decrease earlier than CM $CD4^+$ T-cell counts (2 vs 5 hours after fingolimod exposure; Fig 1, *B*). In $CD8^+$ T cells, contrasting $CD4^+$ T cells, only naive ($CD62L^+CD45RA^+$) $CD8^+$ T-cell counts decreased significantly (after 3 vs 2 hours in naive $CD4^+$ T cells) after the first dose of fingolimod (Fig 1, *C* [representative example; absolute cell counts], and Fig 1, *D* [pooled data; proportional change]).

On the basis of these *ex vivo* depletion kinetics, *in vitro* chemotaxis experiments were performed, as described in the Methods section in this article's Online Repository. In a transwell system spontaneous migration of bulk $CD4^+$ and $CD8^+$ T cells was comparably low in healthy control subjects and untreated patients with MS (and was further decreased in the presence of fingolimod; see Fig E1 in this article's Online Repository at www.jacionline.org). Gradients of CXCL12, CCL19, and CCL21 mediated a clear increase in migration of bulk $CD4^+$ and $CD8^+$ T cells from healthy control subjects and untreated patients with MS, which was not significantly influenced by fingolimod (see Fig E1). Dot plot distribution (as a percentage) of migrated versus nonmigrated, phenotypic naive, CM, EM, and (for $CD8^+$ T cells) CD45RA re-expressing EM cells (EMRA) was then compared between control cells (spontaneous migration) and cells that migrated toward CXCL12, CCL19, or CCL21. An example of CXCL12-mediated changes in the proportional distribution (dot plot) of migrated versus nonmigrated $CD4^+$ T-cell subsets is shown in Fig 2, *A*, whereas Fig E2 (available in this article's Online Repository at www.jacionline.org) shows the distribution of T-cell subsets in the upper wells before and after migration toward CXCL12. Intriguingly, these experiments robustly found that naive $CD4^+$ and $CD8^+$ T cells (from either healthy control subjects and untreated patients with MS) were significantly enriched compared with CM and EM cells (and, in the case of $CD8^+$ cells, also CD45RA re-expressing EM cells, EMRA), indicating enhanced migration in gradients of CXCL12, CCL19, and CCL21 (Fig 2, *B* and *C*). This subset-specific migration pattern was not influenced by the presence of fingolimod (data not shown). In accordance with previous reports, phenotypic naive T cells expressed higher levels of CCR7[7] and CXCR4[8] than their CM counterparts (Fig 2, *D*). Baseline counts of total lymphocytes and T-cell subsets did not differ between healthy control subjects and untreated patients with MS. Also, expression of CCR7 and CXCR4 on T-cell subsets was similar (see Table E2 in this article's Online Repository at www.jacionline.org). In all, these chemotaxis experiments indicate that the LN homing chemokines CXCL12, CCL19, and CCL21 differentially affect migration of naive and CM $CD4^+$ and $CD8^+$ T cells, with preferential chemoattraction induced in naive subsets. Differential S1P responsiveness and thus selective egress of T-cell subsets from secondary lymphoid tissues could also explain the pattern of cellular depletion observed in our clinical study. Although no subset specificity of S1P-mediated *in vitro* migration was observed (see Fig E3 in this article's Online Repository at www.jacionline.org), the low *in vitro* rate of S1P-directed migration, which presumably relates to rapid downregulation of S1P receptor 1 on blood-exposed lymphocytes,[9] limits the extendibility of this observation to an *in vivo* setting.

Together, these data suggest that $CD4^+$ T cells enter lymphoid tissue and thus access DCs more frequently than $CD8^+$ T cells, which might enhance efficient delivery of $CD4^+$ T cell help. Even more pronounced were the differences in calculated homing frequencies between phenotypic naive and antigen-experienced T-cell subsets (2-3 times higher among naive cells, see Table E3 in this article's Online Repository at www.jacionline.org). In line with a higher recirculation frequency *in vivo*, naive $CD4^+$ and $CD8^+$ T cells also migrated *in vitro* more efficiently in gradients of the LN-homing chemokines CCL19/CCL21 and CXCL12. Given the high intrinsic threshold of naive cells to become activated, rapid homing might allow naive T cells to compete for antigen and costimulation, thus reducing the time required for their priming. Also, LN homing of T cells and particularly of naive T cells has recently been linked in mice to cell survival and cellular homeostasis by interaction with fibroblastic reticular cells.[10] The

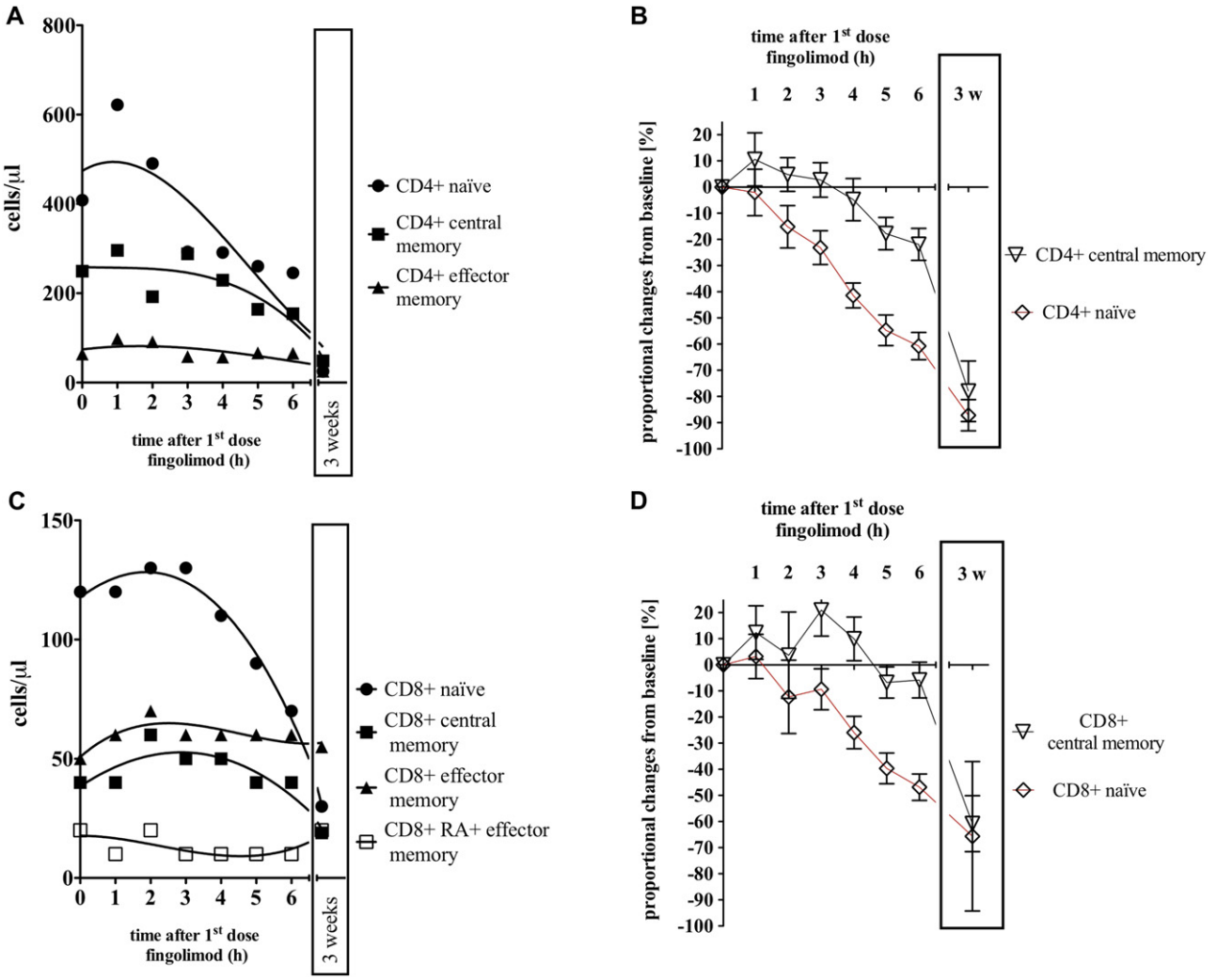

FIG 1. Counts and proportional changes of T-cell subsets in peripheral blood of patients with MS after *de novo* exposure to fingolimod. **A** and **C,** Absolute numbers and trend lines of circulating naive, CM, and EM $CD4^+$ (Fig 1, *A*) and $CD8^+$ (Fig 1, *C*) T cells in a representative patient with MS before and after initiation of treatment with fingolimod. **B** and **D,** Pooled data reflecting the proportional change of circulating naive and CM $CD4^+$ (Fig 1, *B*) and $CD8^+$ (Fig 1, *D*) T cells related to pre-fingolimod values (n = 8, ± SEM).

observed higher frequency of LN homing among naive compared with antigen-experienced cells raises the possibility that similar mechanisms operate in human T cells as well.

In all, by providing an indirect estimate of the LN homing frequency among human T-cell subsets, these data add basic aspects to our understanding of the immune surveillance process.

Matthias Mehling, MD[a,b]
Volker Brinkmann, PhD[c]
Anne-Valerie Burgener, BMSc[a]
Patrick Gubser, MD[a]
Andrew D. Luster, MD, PhD[d]
Ludwig Kappos, MD[b]*
Christoph Hess, MD, PhD[a]*

From [a]the Immunobiology Laboratory/Department of Biomedicine and Medical Outpatient Department and [b]the Department of Neurology and Clinical Neuroimmunology Laboratory/Department of Biomedicine, University Hospital Basel, Basel, Switzerland; [c]the Department of Autoimmunity, Transplantation & Inflammation, Novartis Institutes for BioMedical Research, Basel, Switzerland; and [d]Massachusetts General Hospital, Harvard Medical School, Center for Immunology and Inflammatory Diseases, Charlestown, Mass. E-mail: chess@uhbs.ch.

*These authors contributed equally to this work.

Supported by a grant from Novartis AG, Basel, Switzerland, and by the Swiss Multiple Sclerosis Society. C.H. and P.G. are supported by grants from the Swiss National Science Foundation (31003A_135677/1 and PB323630-128881, respectively).

Disclosure of potential conflict of interest: M. Mehling has received research support from the Novartis Research Foundation and the Swiss MS Society and is employed by University Hospital Basel. V. Brinkmann is employed by Novartis. L. Kappos has received research support from the Novartis Research Foundation (Basel, Switzerland), Bayer, Biogen Idec, Merck Serono, Novartis, Teva, Roche, the Swiss MS Society, the European Union, the Gianni Rubatto Foundation, the Roche Research Foundation, and the Novartis Research Foundation; is a member of the Actelion Data and Safety Monitoring Committee; is on the advisory boards for Advancell, Allozyne, and Wyeth; is chair of the Bayer, Novartis, and Roche Steering Committees; is member and chair of the Biogen Idec advisory board; is chair of the Genmab, MediciNova, Santhera, and UCB Data and Safety Monitoring Committee; is chair of the Merck Serono advisory board; is a member of the Merck Serono Steering Committee; is a member of the Teva advisory board and Steering Committee; has received consultancy fees from Novonordisk, Peptimmune, Glenmark, BioMarin, GeNeuro SA, Eli Lilly, CSL Behring, Bayhill, and Sanofi Aventis; has received lecture fees from Bayer, Biogen Idec, Merck Serono, Novartis, Sanofi Aventis, Roche, and Teva; and has received payment for the development of educational presentations from Bayer, Merck Serono, Novartis, Sanofi Aventis, Roche, Teva, and UCB. C. Hess has received research support from the Swiss National Science Foundation and Research Hub Basel University-Roche and is

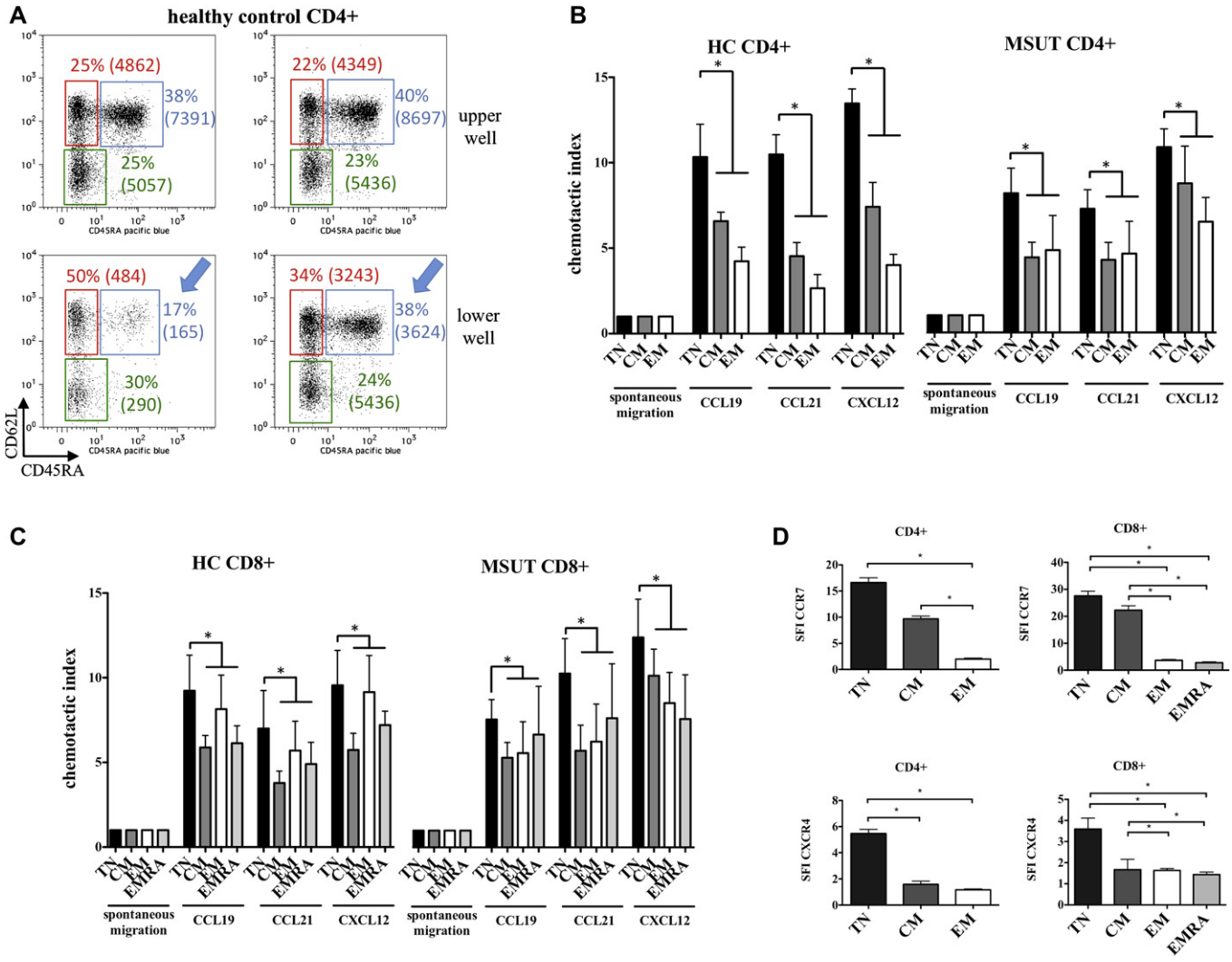

FIG 2. Migration of CD4$^+$ and CD8$^+$ T-cell subsets in gradients of CXCL12, CCL19, or CCL21. **A,** Representative dot plots depicting proportions of CD4$^+$ T-cell subsets and absolute cell counts (in brackets) sampled after migration from the upper and lower wells of a transwell chamber. Note that the increased proportion of naive T cells after migration toward CXCL12 compared with spontaneous migration *(blue arrows)*. **B** and **C,** Chemotactic index values (corrected for background migration) are shown for CD4$^+$ (Fig 2, *B*) and CD8$^+$ (Fig 2, *C*) T-cell subsets that migrated in a gradient of CCL19, CCL21, or CXCL12 (n = 4 per group, ± SEM). **D,** Cell-surface expression of CXCR4 and CCR7 on CD4$^+$ and CD8$^+$ T-cell subsets based on specific fluorescence index (*SFI*; n = 3; ± SEM). **P* < .05. *EMRA*, CD45RA re-expressing effector memory (only in CD8$^+$ T cells); *HC*, healthy control subjects; *MSUT*, untreated patients with MS; *TN*, naive cells.

employed by University Hospital Basel. The rest of the authors declare that they have no relevant conflicts of interest.

REFERENCES

1. Sallusto F, Geginat J, Lanzavecchia A. Central memory and effector memory T cell subsets: function, generation, and maintenance. Annu Rev Immunol 2004;22:745-63.
2. Miyasaka M, Tanaka T. Lymphocyte trafficking across high endothelial venules: dogmas and enigmas. Nat Rev Immunol 2004;4:360-70.
3. Andrian von UH, Mempel TR. Homing and cellular traffic in lymph nodes. Nat Rev Immunol 2003;3:867-78.
4. Matloubian M, Lo CG, Cinamon G, Lesneski MJ, Xu Y, Brinkmann V, et al. Lymphocyte egress from thymus and peripheral lymphoid organs is dependent on S1P receptor 1. Nature 2004;427:355-60.
5. Mehling M, Johnson TA, Antel J, Kappos L, Bar-Or A. Clinical immunology of the sphingosine 1-phosphate receptor modulator fingolimod (FTY720) in multiple sclerosis. Neurology 2011;76(suppl 3):S20-7.
6. Mehling M, Brinkmann V, Antel J, Bar-Or A, Goebels N, Vedrine C, et al. FTY720 therapy exerts differential effects on T cell subsets in multiple sclerosis. Neurology 2008;71:1261-7.
7. Sallusto F, Lenig D, Förster R, Lipp M, Lanzavecchia A. Two subsets of memory T lymphocytes with distinct homing potentials and effector functions. Nature 1999;401:708-12.
8. Lee B, Sharron M, Montaner LJ, Weissman D, Doms RW. Quantification of CD4, CCR5, and CXCR4 levels on lymphocyte subsets, dendritic cells, and differentially conditioned monocyte-derived macrophages. Proc Natl Acad Sci U S A 1999;96:5215-20.
9. Arnon TI, Xu Y, Lo C, Pham T, An J, Coughlin S, et al. GRK2-dependent S1PR1 desensitization is required for lymphocytes to overcome their attraction to blood. Science 2011;333:1898-903.
10. Link A, Vogt TK, Favre S, Britschgi MR, Acha-Orbea H, Hinz B, et al. Fibroblastic reticular cells in lymph nodes regulate the homeostasis of naive T cells. Nat Immunol 2007;8:1255-65.

http://dx.doi.org/10.1016/j.jaci.2012.12.1520

METHODS

Study subjects and procedures

The institutional review board of both cantons of Basel approved the study. Patients starting therapy with fingolimod, untreated patients with MS, and healthy control subjects were recruited to the study between April 2011 and April 2012. Inclusion criteria for patients were as follows: definite relapsing MS, planned therapy with fingolimod (0.5 mg/d), and age between 18 and 65 years. Inclusion criteria for healthy control subjects were the absence of signs, symptoms, or both of acute infection or chronic disease and age between 18 and 65 years. Exclusion criteria for patients were signs, symptoms, or both of acute infection; immunomodulation with IFN-β preparations, glatiramer acetate, or natalizumab; therapy with steroids in the last 3 months or immunosuppression with mitoxantrone or azathioprine 12 months before initiation of fingolimod therapy; and pregnancy. After written informed consent was obtained, blood samples from patients with MS were obtained directly before and hourly for 6 hours after the first dose of fingolimod (0.5 mg), as well as after 3 weeks of treatment with fingolimod (0.5 mg/d).

Flow cytometry

The following antibodies were used: anti-human CD4 peridinin-chlorophyll-protein (SK3), anti-human CD8 phycoerythrin (PE; SK1), anti-human CCR7 PE (3D12), anti-human CXCR4 PE (12G5; all from BD Biosciences, Franklin Lakes, NJ), anti-human CD3 fluorescein isothiocyanate (MEM-57), anti-human CD62L allophycocyanin (LT-TD180; both from Immunotools, Friesoythe, Germany), and anti-human CD45RA pacific blue (2H4; Beckman Coulter, Brea, Calif). As isotype controls, the following antibodies were used: IgG_1-PE (PPV-06), IgG_{2a}-PE (713), IgG_{2a}–fluorescein isothiocyanate (713), IgG_1-allophycocyanin (PPV-06; all from Immunotools), IgG_1–pacific blue (679.1Mc7; Beckman Coulter), and IgG_1-peridinin-chlorophyll-protein (×40; BD Biosciences). All antibodies were titrated individually for use in flow cytometry. A CyAn cytometer (DakoCytomation, Glostrup, Denmark) and a FACSCalibur (Becton Dickinson, Heidelberg, Germany) were used according to standard procedures. Flow cytometric data were analyzed with FlowJo software (TreeStar, Ashland, Ore). Surface expression of CCR7 and CXCR4 was assessed, calculating the specific fluorescence index by dividing the geometric mean fluorescence of the specific antibody by geometric mean fluorescence of the isotype control antibody.

PBMCs and T-cell isolation

PBMCs were isolated by means of Ficoll gradient centrifugation. $CD3^+$ T cells were purified by using positive selection with immunomagnetic bead separation (Miltenyi Biotec, Bergisch Gladbach, Germany). The purity of the isolated $CD3^+$ T-cell population always was greater than 95%.

Migration assay

Isolated $CD3^+$ T cells were resuspended at 4×10^6 cells/mL in RPMI 1640 containing 10% FCS, 50 U/mL penicillin, and 50 mg/mL streptomycin (R10; all from Life Technologies, Carlsbad, Calif). $CD3^+$ T cells (6×10^5) were resuspended in the presence or absence of pertussis toxin (100 ng/mL) for inhibition of G protein–coupled chemokine receptors, such as CXCR4 or CCR7[E1] (Life Technologies) or fingolimod/phosphorylated fingolimod (10 nmol/L each), and were loaded in duplicates into uncoated 6.5-mm-diameter, 5-μm pore-size polycarbonate transwell inserts (Costar, Corning, NY). One milliliter of R10 or solutions of CCL19 (100 nmol/L), CCL21 (100 nmol/L; both from PeproTech, Rocky Hill, NJ), or CXCL12 (5 nmol/L; R&D Systems, Minneapolis, Minn) were added to the lower well, and cells were incubated for 6 hours at 37°C in 5% CO_2. For assessment of S1P-directed migration, S1P (10 nmol/L; Enzo Life Sciences, Farmingdale, NY) was added to the lower well, and cells were incubated for 3 hours at 37°C in 5% CO_2. After incubation, cells from the upper and lower wells were counted with a FACSCalibur and stained for flow cytometry. The chemotactic index indicates the proportion of cells initially plated in the upper well that migrated to the lower well and was determined by dividing absolute cell counts of migrated cells by absolute cell counts of input cells in the upper well.

Calculation of LN homing frequencies

The homing rate or frequency *(f)* was assumed to be unchanged before and after the first dose of fingolimod. The egress rate *(e′)* of a given peripheral blood T-cell subset *(PT)* is denoted as $e'PT$. The change in numbers of a given peripheral blood T-cell subset over time thus relates to homing rate and egress rate as follows:

$$\frac{\Delta PT}{\Delta t} = f - e'PT.$$

On the basis of changes (Δ values) of given peripheral blood T-cell subsets 6 hours after the first dose of fingolimod, in a conservative estimate (conservative because egress is not blocked immediately after the first dose of fingolimod),[E2] the daily LN homing rate or frequency (f_d) corresponds to the following:

$$f_d = \left[\frac{\Delta PT_{6h}}{6}\right] \times 24.$$

Statistical analysis

Data were tested for normality with the Shapiro-Wilk test. Data with normal distribution were assessed by using the Student 2-sided *t* test, and data with nonnormal distribution were assessed by using the Wilcoxon test. *P* values of less than .05 were considered statistically significant.

REFERENCES

E1. Phillips R, Ager A. Activation of pertussis toxin-sensitive CXCL12 (SDF-1) receptors mediates transendothelial migration of T lymphocytes across lymph node high endothelial cells. Eur J Immunol 2002;32:837-47.

E2. Kovarik JM, Schmouder R, Barilla D, Riviere GJ, Wang Y, Hunt T. Multiple-dose FTY720: tolerability, pharmacokinetics, and lymphocyte responses in healthy subjects. J Clin Pharmacol 2004;44:532-7.

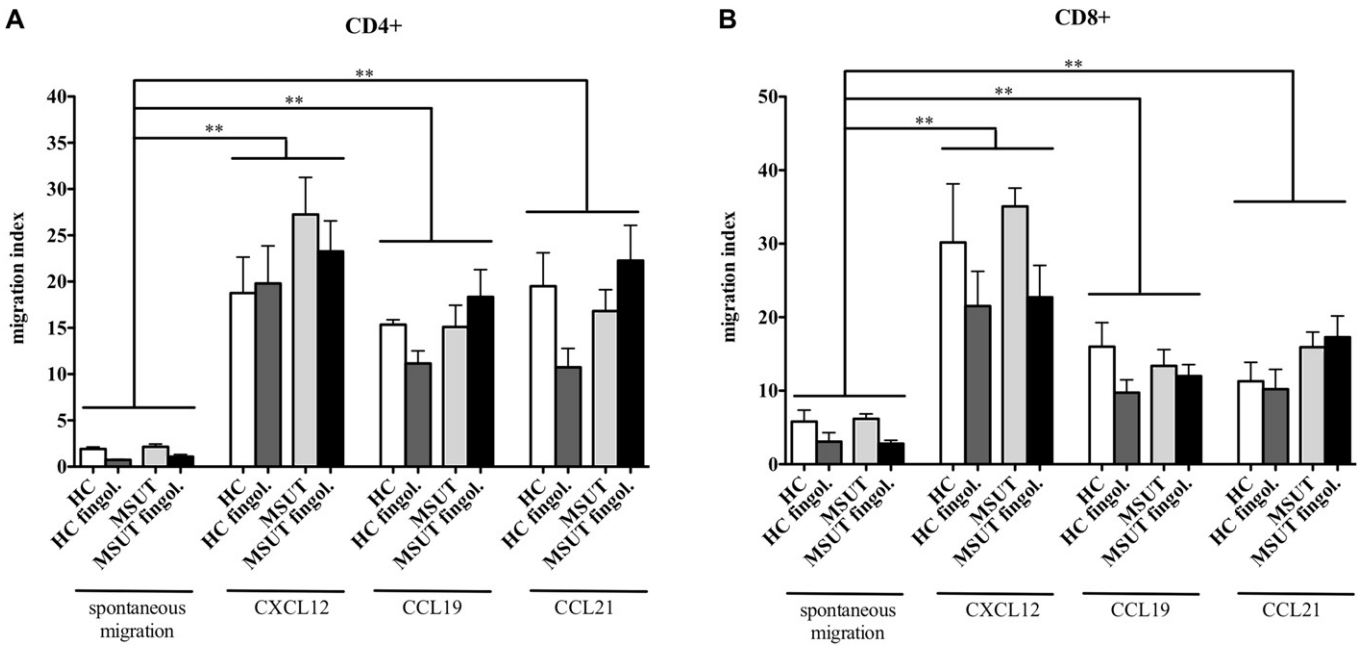

FIG E1. Migration of bulk $CD4^+$ and $CD8^+$ T cells in gradients of CXCL12, CCL19, and CCL21. **A,** Proportion (chemotactic index) of bulk $CD4^+$ T cells migrating spontaneously or toward the LN homing chemokines CXCL12, CCL19, and CCL21 (n = 4 per group, ± SEM). **B,** Proportion of bulk $CD8^+$ T cells migrating spontaneously or toward the LN homing chemokines CXCL12, CCL19, and CCL21 (n = 4 per group, ± SEM). *HC*, Healthy control subjects; *MSUT*, untreated patients with MS; *fingol.*, input cells pretreated with fingolimod/fingolimod-P. $^{**}P < .001$.

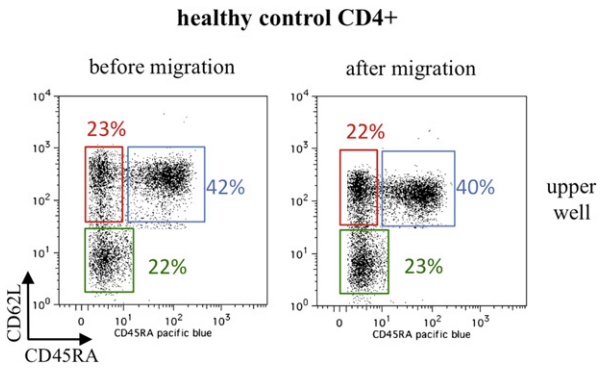

FIG E2. Proportional distribution of T-cell subsets from the upper well of a representative transwell migration assay before and after exposure to CXCL12. Representative *dot plots* depicting proportions of phenotypic naive ($CD45RA^{+}CD62L^{+}$), CM ($CD45RA^{-}CD62L^{+}$), and EM ($CD45^{-}CD62L^{-}$) $CD4^{+}$ T cells sampled before and after migration from the upper well of a transwell chamber.

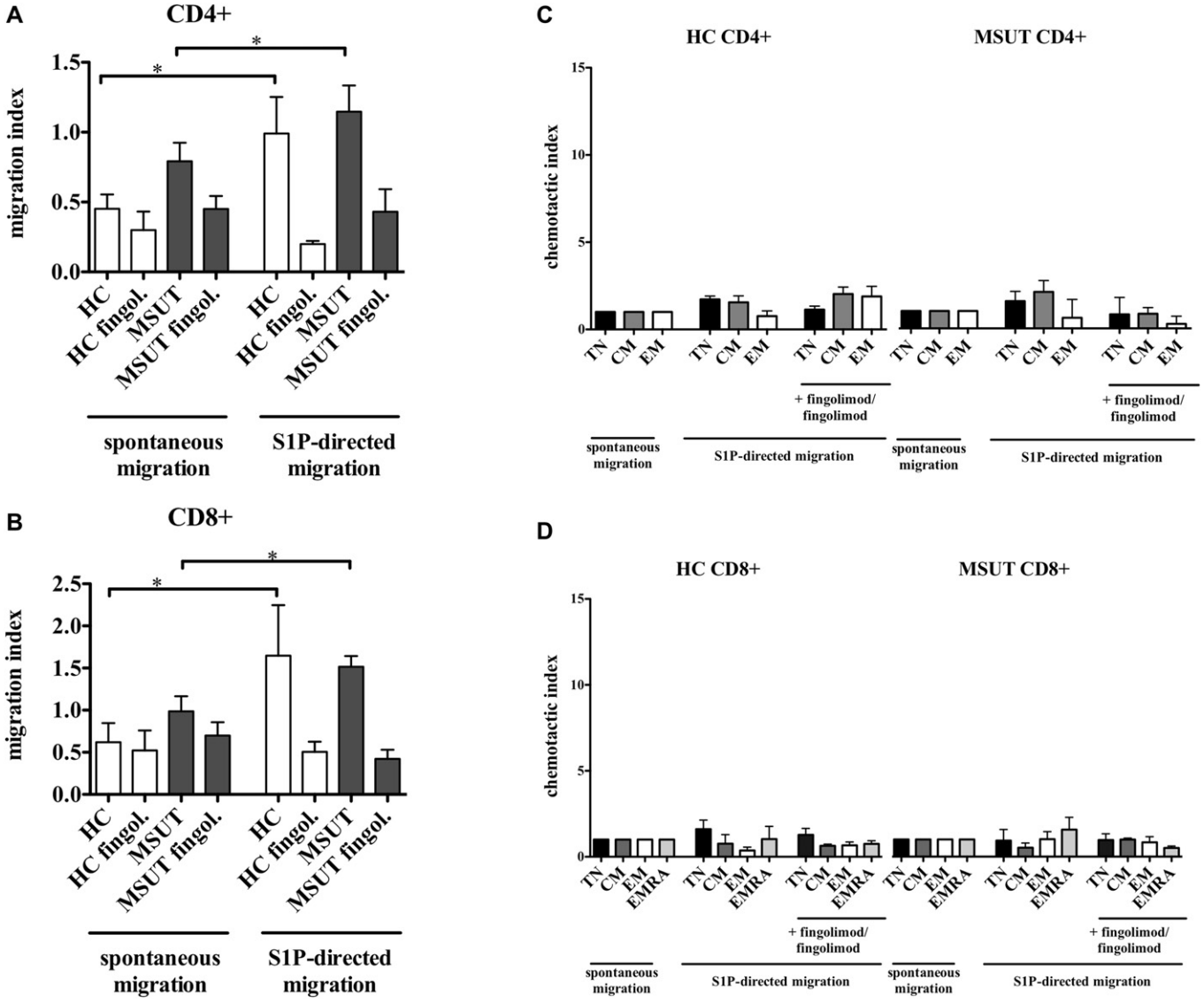

FIG E3. Migration of $CD4^+$ and $CD8^+$ T cells in gradients of S1P. **A,** Proportion (chemotactic index) of bulk $CD4^+$ T cells migrating spontaneously or toward S1P. Note that S1P-directed migration was abrogated in $CD4^+$ T cells pretreated with fingolimod (n = 3 per group; ± SEM). **B,** Proportion (chemotactic index) of bulk $CD8^+$ T cells migrating spontaneously or toward S1P. Note that S1P-directed migration was abrogated in $CD8^+$ T cells pretreated with fingolimod (n = 3 per group; ± SEM). **C,** The distribution of $CD4^+$ T-cell subsets that migrated in a gradient of S1P is shown related to the distribution of these same subsets among spontaneously migrating cells (n = 3 per group; ± SEM). **D,** The distribution of $CD8^+$ T-cell subsets that migrated in a gradient of S1P is shown related to the distribution of these same subsets among spontaneously migrating cells (n = 3 per group; ± SEM). *EMRA*, CD45RA re-expressing effector memory (only in $CD8^+$ T cells); + *fingolimod/fingolimod-P*, cells pretreated with these compounds; *HC*, healthy control subjects; *MSUT*, untreated patients with MS; *TN*, naive cells. **P* < .05.

TABLE E1. Characteristics of the study population

	Patients with MS	Healthy control subjects
No.	14	7
Median age (y) [range]	49 [35-58]	38 (33-44)
Female/male sex	9/5	5/2
Median disease duration (y) [range]	14 [3-23]	NA
Median EDSS	4.75	NA

EDSS, Expanded Disability Status Scale; *NA*, not applicable.

TABLE E2. Cell counts and expression of CCR7 and CXCR4 (specific fluorescence index) among healthy control subjects (n = 4) and untreated patients with MS (n = 8 for lymphocyte counts and n = 4 for expression levels of CCR7 and CXCR4)

	HC		MSUT		
	Mean	**SD**	**Mean**	**SD**	***P* value**
Cells/μL					
Total lymphocytes	1600	416	1450	649	.53
Total $CD4^+$ T cells	638	138	712	298	.92
$CD4^+$ naive	240	88	208	204	.78
$CD4^+$ CM	240	80	339	132	.28
$CD4^+$ EM	160	60	92	53	.19
Total $CD8^+$ T cells	345	25	275	248	.63
$CD8^+$ naive	120	17	105	128	.41
$CD8^+$ CM	56	13	70	113	.19
$CD8^+$ EM	82	22	60	45	.92
$CD8^+$ EMRA	60	8	35	69	.41
SFI CCR7					
$CD4^+$ naive	17.0	1.9	18.6	4.5	.68
$CD4^+$ CM	9.8	1.1	13.5	3.0	.22
$CD8^+$ naive	27.2	3.5	34.6	2.9	.16
$CD8^+$ CM	22.4	3.3	28.9	7.3	.34
SFI CXCR4					
$CD4^+$ naive	5.2	0.4	6.3	0.4	.37
$CD4^+$ CM	1.8	0.1	1.2	0.1	.81
$CD8^+$ naive	3.9	1.1	3.5	0.7	.78
$CD8^+$ CM	1.2	0.1	2.6	1.4	.65

EMRA, CD45RA re-expressing EM ($CD8^+$ T cells only); *HC*, healthy control subjects; *MSUT*, untreated patients with MS; *SFI*, specific fluorescence index.

TABLE E3. Estimated homing frequencies of T-cell subsets

Subset	Percentage decrease after 6 h	Estimated homing frequency/d
$CD4^+$ naive	−60.7 (SEM 5.2)	2.4
$CD4^+$ CM	−21.9 (SEM 2.8)	0.9
$CD8^+$ naive	−46.7 (SEM 5.1)	1.9
$CD8^+$ CM	−5.9 (SEM 6.4)	<0.9

Proportional decrease (in percentages) of naive and CM $CD4^+$ and $CD8^+$ T cells 6 hours after the first dose of fingolimod (n = 8) and derived estimates of respective homing frequencies are shown.